A new juvenile sauropod specimen from the Middle Jurassic Dongdaqiao Formation of East Tibet

Xianyin An [1] , **Xing Xu** [2, 3, 4] , **Fenglu Han** [Corresp., 5] , **Corwin Sullivan** [6, 7] , **Qiyu Wang** [1] , **Yong Li** [1] , **Dongbing Wang** [1] , **Baodi Wang** [1] , **Jinfeng Hu** [5]

[1] Chengdu Center of China Geological Survey, Chengdu, Sichuan, China
[2] Key Laboratory of Vertebrate Evolution and Human Origins, Institute of Vertebrate Paleontology and Paleoanthropology,, China Academy of Sciences, Beijing, China
[3] Center for Excellence in Life and Paleoenvironment, Chinese Academy of Sciences, Beijing, China
[4] Centre for Vertebrate Evolutionary Biology, Yunnan University, Kunming, Yunnan, China
[5] School of Earth Sciences, China University of Geosciences (Wuhan), Wuhan, Hubei, China
[6] Department of Biological Sciences, University of Alberta, Edmonton, Canada
[7] Philip J. Currie Dinosaur Museum, Wembley, Canada

Corresponding Author: Fenglu Han
Email address: hanfl@cug.edu.cn

Jurassic strata are widely distributed in the eastern part of Tibet Autonomous Region, and have yielded many dinosaur bones. However, none of these specimens has been studied extensively, and some remain unprepared. Here we provide a detailed description of some new sauropod material, including several cervical vertebrae and a nearly complete scapula, recovered from the Middle Jurassic of Chaya County, East Tibet. The cervical vertebrae have short centra that bear ventral midline keels, as in other early-diverging eusauropods such as *Shunosaurus*. Moreover, the cervical centra display deep lateral excavations, partitioned by a septum. The scapula has proximal and distal ends that are both expanded as in mamenchisaurids and neosauropods. However, relatively small body size and lack of fusion of neurocentral sutures in the cervical vertebrae suggest that the available material is from a juvenile, and the length of the cervical centra may have increased relative to the size of the rest of the skeleton in later ontogenetic stages. The new Tibetan sauropod specimens provide important information on the morphological transition between *Shunosaurus* and mamenchisaurids, and extend the known biogeographic range of early-diverging sauropods in the Middle Jurassic of East Asia.

A new juvenile sauropod specimen from the Middle Jurassic Dongdaqiao Formation of East Tibet

Xianyin An[1], Xing Xu[2,3,4], Fenglu Han[5*], Corwin Sullivan[6,7], Qiyu Wang[1], Yong Li[1], Dongbing Wang[1], Baodi Wang[1], Jinfeng Hu[5]

[1] Chengdu Center of China Geological Survey, Chengdu, Sichuan, China
[2] Key Laboratory of Vertebrate Evolution and Human Origins, Institute of Vertebrate Paleontology and Paleoanthropology, Chinese Academy of Sciences, Beijing, China
[3] Center for Excellence in Life and Paleoenvironment, Chinese Academy of Sciences, Beijing, China
[4] Centre for Vertebrate Evolutionary Biology, Yunnan University, Kunming, China
[5] School of Earth Sciences, China University of Geosciences (Wuhan), Wuhan, China
[6] Department of Biological Sciences, University of Alberta, Edmonton, Canada
[7] Philip J. Currie Dinosaur Museum, Wembley, Canada

Corresponding Author:
Fenglu Han[5]
Lumo Road, Wuhan, Hubei Province, 430074, China
Email address: hanfl@cug.edu.cn

Abstract

Jurassic strata are widely distributed in the eastern part of Tibet Autonomous Region, and have yielded many dinosaur bones. However, none of these specimens has been studied extensively, and some remain unprepared. Here we provide a detailed description of some new sauropod material, including several cervical vertebrae and a nearly complete scapula, recovered from the Middle Jurassic of Chaya County, East Tibet. The cervical vertebrae have short centra that bear ventral midline keels, as in other early-diverging eusauropods such as *Shunosaurus*. Moreover, the cervical centra display deep lateral excavations, partitioned by a septum. The scapula has proximal and distal ends that are both expanded as in mamenchisaurids and neosauropods. However, relatively small body size and lack of fusion of neurocentral sutures in the cervical vertebrae suggest that the available material is from a juvenile, and the length of the cervical

centra may have increased relative to the size of the rest of the skeleton in later ontogenetic stages. The new Tibetan sauropod specimens provide important information on the morphological transition between *Shunosaurus* and mamenchisaurids, and extend the known biogeographic range of early-diverging sauropods in the Middle Jurassic of East Asia.

Introduction

In Tibet, the highest-altitude region in the world, a series of Jurassic-Cretaceous strata are exposed in the eastern part of Changdu (Qamdo) Prefecture. In the 1970s, the Scientific Expedition Team of the Chinese Academy of Sciences discovered many Early-Middle Jurassic dinosaur bones in this area, representing at least ten species and including sauropodomorph, theropod, stegosaur, and early-diverging ornithischian remains (*Zhao, 1985; An et al., 2021*). Almost all these specimens are still unpublished, the sole exception being the partial, medium-sized stegosaur skeleton, comprising the iliosacral region together with two incomplete vertebrae and three dermal plates, that was made the holotype of *Monkonosaurus lawulacus* (*Zhao, 1983; Dong, 1990*). However, this species is probably a *nomen dubium* (*Maidment & Wei, 2006*). Some sauropod dinosaur trackways were also reported in the Jurassic of Changdu, and at least 10 track sites have been discovered (*Xing, Harris & Currie, 2011; Xing et al., 2021*). The wide gauge of some of the tracks suggest that large sauropods lived in the Early-Middle Jurassic of this area and may have been closely related to the very abundant sauropods from the Jurassic of the Sichuan Basin, of which about 30 species have been established. Three distinct Jurassic sauropod faunas have been defined within the Sichuan Basin, namely the Early Jurassic *Zizhongosaurus* Fauna, the Middle Jurassic *Shunosaurus*-*Omeisaurus* Fauna and the Late Jurassic *Mamenchisaurus* Fauna (*Li, 1998*).

In 2019, the field team of the Chengdu Center of the China Geological Survey discovered some new dinosaur fossil sites in Chaya County, Changdu District, Tibet, and collected and prepared some sauropod bones (*An et al., 2021*). Here we give a detailed description of this material and draw comparisons with other sauropods from Gondwana and Laurasia. Our new material may have significant implications for understanding the evolution and diversity of early sauropods in the Jurassic of East Asia.

Materials & Methods

The sauropod specimens described in this paper are postcranial elements, and are housed at the Chengdu Center of the China Geological Survey (CGS V001). They include four cervical vertebrae and a nearly complete scapula. All these bones were found together within a small area and are likely to be from one individual, though none were preserved in articulation. Field activities were approved by Chengdu Geological Survey Center (project number: DD20190053).

Measurements of the bones are given in Table 1. High-resolution 3D models of the cervical vertebrae and scapula have been uploaded to datadryad.org (doi:10.5061/dryad.f7m0cfz16). All the bones were scanned using an Artec Space Spider hand-held 3D scanner from China University of Geosciences, and the scans were edited to produce final 3D models using the software Artec Studio.

Phylogenetic analysis. To assess the systematic position of our new Tibetan sauropod, we scored it into a recent data matrix for early-diverging sauropods (*Ren et al., 2021*), derived from a previously published matrix (*Xu et al., 2018*). The new matrix contains 386 characters and 77 taxa. Only 30 characters could be scored for the Tibetan sauropod, due to poor preservation. The new matrix was analyzed using TNT v1.5 (*Goloboff & Catalano, 2016*). All characters were treated as equally weighted. 26 characters (12, 58, 95, 96, 102, 106, 108, 115, 116, 119, 120, 145, 152, 163, 213, 216, 232, 233, 234, 235, 252, 256, 298, 299, 301, 379) were treated as ordered, following the original analysis (*Ren et al., 2021*). The maximum number of stored trees was set to 10,000. A New Technology search was performed with default settings, and hit the best score 50 times. The resulting trees were subjected to a Traditional search using the TBR Swapping algorithm, in order to obtain a final set of most parsimonious trees.

Institutional abbreviations. CLGPR, Chongqing Laboratory of Geoheritage Protection and Research; **LM**, Lingwu Museum; **ZDM,** Zigong Museum; **MCDUT,** Museum of Chengdu University of Technology.

Geological setting

The specimens described in this paper were discovered in Qamdo District, about 10 km from urban center of Chaya County (Fig. S1). Jurassic strata form an extensively exposed succession in the Qamdo Basin, and mainly comprise lacustrine deposits. The Jurassic strata of the Qamdo Basin include the Lower Jurassic Wangbu Formation, the Middle Jurassic Dongdaqiao Formation, and the Upper Jurassic Xiaosuoka Formation. The new specimens are from the Dongdaqiao Formation, which is about 1.2 km thick and mainly consists of purple red feldspar and quartz-bearing sandstones and siltstones. The dinosaur bones were recovered from red argillaceous siltstone in the middle part of the formation, within a thickness of about 5 m (Fig. 1). The Dongdaqiao Formation has generally been considered to date from the Middle Jurassic, based on its bivalve assemblage (*Wang & Chen, 2005*).

Results

Systematic paleontology

Saurischia Seeley, 1887
Sauropodomorpha Huene, 1932
Sauropoda Marsh, 1878
Eusauropoda Upchurch 1995

Description.
Four isolated cervical vertebrae, including an axis, have been prepared. The centra are relatively short, with an average elongation index (aEI: ratio of centrum length to the average of centrum height and width) of about 1.5-2.1 (Table 1). The equivalent ratio is similar in *Shunosaurus* (2.0-3.0) from the Middle Jurassic of Sichuan Basin (*Zhang, 1988*), *Tazoudasaurus* (1.6) and *Barapasaurus* (about 2) from the Early Jurassic of India (*Allain & Aquesbi, 2008; Bandyopadhyay et al., 2010*), and *Patagosaurus* (1-1.7) from the Middle Jurassic of Argentina (*Holwerda, Rauhut & Pol, 2021*), but larger in *Cetiosaurus* (2.3-2.7), *Bagualia* (3.8-5.3) (*Pol et al., 2020; Gomez, Jose & Pol, 2021; Holwerda, Rauhut & Pol, 2021*), and mamenchisaurids such as *Analong* (*Ren et al., 2021*) and *Omeisaurus tianfuensis* (1.9-6.1) (*He, Li & Cai, 1988*). The lateral surfaces of the three postaxial cervical centra bear pleurocoels that are partitioned by anterodorsally-trending ridges, as in some cervical vertebrae of *Patagosaurus* (*Holwerda, Rauhut & Pol, 2021*), mamenchisaurids and neosauropods (*Wilson, 2002*). A ventral midline keel is present on the anterior part of each centrum as in the cervical vertebrae of many early-diverging sauropods, such as *Shunosaurus* (*Zhang, 1988*), *Tazoudasaurus* (*Allain & Aquesbi, 2008*), *Omeisaurus* (*He, Li & Cai, 1988*), *Lingwulong* (*Xu et al., 2018*), *Patagosaurus* (*Holwerda, Rauhut & Pol, 2021*), *Bagualia* (*Gomez, Jose & Pol, 2021*), , *Spinophorosaurus* (*Remes et al., 2009*), *Lapparentosaurus* (*Upchurch, 1998*), *Amygdalodon* (*Rauhut, 2003*), an unnamed sauropod from Morocco (*Nicholl, Mannion & Barrett, 2018*), and the anteriormost cervicals of the Rutland *Cetiosaurus* (*Upchurch & Martin, 2002*). This feature is also present in some non-sauropod sauropodomorphs, including *Yizhousaurus* (*Zhang et al., 2018*),

Massospondylus (*Barrett et al., 2019*), *Isanosaurus* (*Buffetaut et al., 2000*), and potentially *Antetonitrus* (*McPhee et al., 2014*), and *Lamplughsaura* (*Kutty et al., 2007*).

Axis. The axis (CGS V001-1) is nearly complete, and is well preserved (Fig. 2), with a length of 12.6 cm. The anterior surface of the axis is rugose, bears a pair of dorsoventral grooves, and is tilted to face somewhat dorsally (Fig. 2C). The odontoid process is not preserved. The ventral part of the anterior part of the centrum contacts, and is fused with, the axial intercentrum (ic) (Fig. 2A). The latter is a small, irregular bone with a crescentic outline in anterior view (Fig. 2C). The ventral surface is smooth and curved dorsally.

The centrum of the axis is relatively elongate (aEI value of 1.5), and transversely compressed. In anterior view, the centrum is taller than wide (Fig. 2C). The posterior surface of the centrum is strongly concave, accommodating the anterior condyle of the third cervical centrum, and has a subcircular outline with equal width and height. The lateral surface of the centrum bears a shallow, elongate fossa with poorly defined margins and no external pneumatic openings, as in the early-diverging eusauropods *Shunosaurus* (*Zhang, 1988*) and *Bagualia* (*Gomez, Jose & Pol, 2021*), whereas the corresponding fossa is deeper in more derived sauropods such as *Omeisaurus* (*He, Li & Cai, 1988*) and *Euhelopus* (*He, Li & Cai, 1988; Wilson & Upchurch, 2009*). The fossa is deepest at the anterior end, and gradually becomes shallower posteriorly. The fossa is undivided, as in *Shunosaurus* (*Zhang, 1988*), *Cetiosaurus* (*Upchurch & Martin, 2002*), *Bagualia* (*Gomez, Jose & Pol, 2021*), *Mamenchisaurus* (*Yang & Dong, 1972*) and *Xinjiangtitan* (*Zhang et al., 2020*), whereas the lateral fossa on the axis is partitioned by a ridge in *Omeisaurus* (*He, Li & Cai, 1988*) and more derived sauropods. The parapophysis, positioned on the anterior margin of the centrum, is a weakly developed structure that takes the form of a convex ridge (Fig. 2A and 2C).

The posterior half of the ventral surface has a gentle transverse convexity. The anterior half of the centrum narrows ventrally but does not form a sharp midline keel of the kind seen in some non-sauropod sauropodomorphs (e.g. *Yizhousaurus* (*Zhang et al., 2018*)) and such early diverging sauropods as *Shunosaurus* (*Zhang, 1988*), *Tazoudasaurus* (*Allain & Aquesbi, 2008*) and *Bagualia* (*Gomez, Jose & Pol, 2021*). The ventral surface of the axis is flat and lacks a midline keel in *Barapasaurus* (*Bandyopadhyay et al., 2010*) and *Mamenchisaurus* (*Yang & Dong, 1972*). In the mamenchisaurid *Xinjiangtitan*, the anterior part of the ventral surface of the axial centrum lacks a keel but bears paired fossae whose outer margins are defined by ventrolateral ridges (*Zhang et al., 2020*).

The neural arch is well developed, but less dorsoventrally tall than the centrum in the mid-region of the vertebra. The part of the neural arch anterior to the apex of the neural spine is taller than the part posterior to the apex (Fig. 2C, F). Both diapophyses are largely broken away, but the bases of these structures are anteroposteriorly elongate and located anteroventrally on the neural arch, just above the neurocentral suture (Fig. 2B). No posterior centrodiapophyseal lamina (pcdl) is observable. The anterior opening of the neural canal is large, and taller than wide (Fig. 2C), whereas the posterior opening is relatively small and subcircular, with equal width and height (Fig. 2F; Table 1).

The prezygapophyses are not preserved. The postzygapophyses are large, and extend posterolaterally beyond the posterior part of the centrum. The postzygodiapophyseal lamina (podl) forms a weak ridge extending posterodorsally at an angle of about 30° above the horizontal (Fig. 2A, B). A large spinopostzygapophyseal fossa (spof) is present between the postzygapophyses (Fig. 2F), as in *Xinjiangtitan* (*Zhang et al., 2020*). The postzygapophyseal articular facets face ventrally, and are elliptical in outline. The long axis of each facet diverges at 45° from that of the centrum. A prominent epipophysis is clearly present on the dorsal surface of the postzygapophysis (Fig. 2A, 2B, and 2F), as in *Bagualia* (*Gomez, Jose & Pol, 2021*) and *Xinjiangtitan* (*Zhang et al., 2020*). The epipophysis is essentially a dorsal extension of the postzygapophysis, but is separated from the main dorsal surface of the latter by a shallow groove.

The neural spine is weakly developed. The anterior part of the spine is transversely narrow, but a robust ridge runs along the dorsal margin of this portion of the spine and is thick enough to slightly overhang a deep, distinct fossa (spinodiapophyseal fossa, sdf) situated on the spine's lateral surface, as in the mamenchisaurids *Mamenchisaurus hochuanensis* (*Yang & Dong, 1972*) and *Xinjiangtitan shanshanensis* (*Zhang et al., 2020*). The fossa is slightly deeper than that of *Bagualia* (*Gomez, Jose & Pol, 2021*), whereas in *Tazoudasaurus* and the Rutland *Cetiosaurus* the lateral surface of the neural spine is flattened or convex (*Upchurch & Martin, 2002; Allain & Aquesbi, 2008*). The height of the neural spine gradually increases posteriorly, reaching a maximum slightly posterior to the midpoint of the centrum as in *Shunosaurus* (*Zhang, 1988*) and *Mamenchisaurus* (*Yang & Dong, 1972*). In *Tazoudasaurus* and the Rutland *Cetiosaurus*, by contrast, the apex of the neural spine is near the posterior margin of the centrum (*Upchurch & Martin, 2002; Allain & Aquesbi, 2008*). The spinopostzygapophyseal lamina (spol) is straight and robust, and trends ventrolaterally.

Postaxial cervical vertebrae. A nearly complete cervical vertebra (CGS V001-2) is well preserved, except that the anterior left half and posterior portion of the neural arch are missing, and the left half of the posterior portion of the centrum has been broken away (Fig. 3). The cervical centrum is strongly opisthocoelous, with a prominent hemispherical anterior condyle. The centrum is about 196 mm long, and the ratio of centrum length to posterior centrum height is about 1.9. The posterior articular surface is tilted to face partly ventrally, rather than being perpendicular to the long axis of the centrum. The parapophyses are missing, owing to damage to the anteroventral part of the centrum. The relatively modest height of the preserved neural arch, and the small size of the centrum as a whole, suggest that this vertebra may be from the anterior part of the cervical series.

The lateral surface of the centrum is strongly excavated by a long depression. A thin, sharp, anterodorsally-trending septum (plr) divides the depressed area into two deep pleurocoels (Fig. 3A and 3B). The anterior pleurocoel extends into the centrum in all directions, except posteriorly. The external opening of the anterior pleurocoel is elliptical and anteroposteriorly elongate, whereas the posterior fossa is relatively shallow and subcircular. The ventral surface of the centrum is strongly concave anteroposteriorly, and slightly concave transversely. The ventral surface bears two shallow fossae anteriorly and is transversely concave posteriorly, but bears a shallow midline keel along its full length.

On the right side of the neural arch, the distal end of the diapophysis is missing, but the basal part of the diapophysis is flattened dorsoventrally, with a thick mid-region and thin anterior and posterior margins. The diapophysis projects laterally and slightly ventrally, and is supported by a well-developed anterior centrodiapophyseal lamina (acdl), which is stout and oriented posterodorsally (Fig. 3A). The partially preserved prezygodiapophyseal lamina (prdl) extends anterodorsally from the diapophysis to the ventrolateral surface of the prezygapophysis (Fig. 3D). The postzygodiapophyseal lamina (podl) is flattened transversely and tapers posterodorsally.

The prezygapophyses are broken away, but a stout, vertically aligned centroprezygapophyseal lamina (cprl) is preserved on the right side of the neural arch (Fig. 3E). An intraprezygapophyseal lamina (tprl) extends ventromedially from the prezygapophysis towards the middle of the dorsal edge of the neural canal. The centroprezygapophyseal lamina (cprl) and intraprezygapophyseal lamina (tprl) combine dorsally forming a large, deep fossa. A deep elliptical fossa is present between the diapophysis and the anterior centrodiapophyseal lamina (acdl) on the lateral side of the neural arch (Fig. 3A). The postzygapophyses are not preserved, and most of the neural spine is likewise missing. The anterior side of the base of the neural spine is incised by a deep, wide vertical groove (Fig. 3E). A robust spinoprezygapophyseal lamina (sprl) is preserved on the right side, and extends posteriorly, medially and slightly dorsally from the prezygapophyseal area to the neural spine (Fig. 3D).

A second postaxial cervical vertebra is well preserved, but the anterior part, and much of the right side, of the centrum are missing (CGS V001-3, Fig. 4). The relatively large size and well-developed neural spine suggest that this vertebra may be from the mid-cervical region. The left lateral surface is excavated by a shallow, elliptical, anteroposteriorly elongate pleurocoel (Fig. 4B). A stout, anterodorsally oriented ridge (plr) forms the pleurocoel's anterior margin. A second pleurocoel was probably originally present anterior to this ridge, as in mamenchisaurid and neosauropod cervical vertebrae. Based on the position of the ridge in typical cervicals, in fact, it is likely that the anterior half of the centrum is missing. The ventral part of the right half of the centrum is similarly broken away to expose the centrum's internal structure. A large, anteroposteriorly elongate pleurocoel is present (Fig. 4A) as in other early-diverging eusauropods such as *Camarasaurus* (*Wedel, 2003*), but lacks the camellate internal cavities that occur in derived titanosaurs. The preserved part of the ventral surface is obviously concave both transversely and anteroposteriorly. The preserved part of the centrum lacks a prominent ventral keel, but a ventral keel may have been present more anteriorly, as in the cervical vertebrae of other early-diverging sauropods and some massopodans.

On the left side of the neural arch, the diapophysis is well preserved, has a subtriangular outline in dorsal view, and tapers ventrolaterally (Fig. 4B). The dorsal surface of the diapophysis is flattened. The prezygodiapophyseal lamina (prdl) is partially preserved as a sheet of bone arising from the base of the anterior edge of the diapophysis, with a thin edge that extends anterodorsally (Fig. 4B). The postzygodiapophyseal lamina (podl) runs from the base of the diapophysis to the lateral margin of the postzygapophysis, forming an angle of about 40° with the long axis of the centrum (Fig. 4B). A prominent, tapering process protrudes posteroventrally from the base of the diapophysis (Fig. 4B: ppr), resembling the costal spurs present in the neosauropod *Euhelopus zdanskyi*. However, the costal spurs of *Euhelopus* are less prominent and more distally located (*Wilson & Upchurch, 2009*).

Both the pre- and postzygapophyses are missing. The spinoprezygapophyseal lamina (sprl) is sharp, its margin curving posterodorsally from the prezygapophyseal area to merge with the anterior edge of the neural spine (Fig. 4B). The neural spine is well preserved, subrectangular in outline in lateral view, and transversely compressed. The anterior neural spine groove is present and transversely narrow. In posterior view, the spinopostzygapophyseal fossa (spof) is deep and tall (Fig. 4C). The neural canal is subcircular and much smaller than the posterior surface of the centrum.

A third postaxial cervical vertebra can be recognized as a posterior member of the cervical series, based on the relative shortness of the centrum and pleurocoel (ratio of centrum length to posterior centrum height of only about 1.68) (CGS V001-4, Fig. 5). The centrum is strongly opisthocoelous, with a prominent hemispherical anterior condyle. The lateral surface of the centrum is strongly excavated by a deep, elliptical pleurocoel (Fig. 5A). The right parapophysis is broken away, but the left parapophysis is located on the anteroventral region of the centrum and tapers laterally, having a triangular outline in lateral and anterior views (Fig. 5B).

The ventral surface is strongly concave anteroposteriorly, the apex of the concavity being located in the anterior half of the centrum. A strong ventral midline keel is present, and extends along the entire length of the centrum. The midline keel is sharp and deep anteriorly, and progressively becomes wider and less prominent towards the centrum's posterior end (Fig. 5D). The centroprezygapophyseal lamina (cprl) is a simple stout ridge, extending anterodorsally from the diapophysis to support the prezygapophysis (Fig. 5C).

The left prezygapophysis is well preserved, with a subtriangular facet that faces dorsomedially and is teardrop-shaped, tapering posteromedially to a point. The articular surface is flattened. A large, shallow fossa is present on the underside of the prezygapophysis (Fig. 5C). The spinoprezygapophyseal lamina (sprl) forms a prominent ridge extending posterodorsally from the prezygapophysis (Fig. 5A). The diapophysis and the posterior part of the prezygodiapophyseal lamina (prdl) are broken away. The anterior part of the prezygodiapophyseal lamina (prdl) is preserved as a stout ridge, whereas the postzygodiapophyseal lamina (podl) appears thinner and more sheet-like, based on the preserved basal part of the latter (Fig. 5B, E). The anterior centrodiapophyseal lamina (acdl) is thick and extends posterodorsally, and the posterior centrodiapophyseal lamina (pcdl) extends anterodorsally. Together with the dorsal lamina on the centrum (dlc), they define a deep fossa situated ventral to the diapophysis and visible in lateral view (Fig. 5B) as in the posterior cervical vertebrae of *Europasaurus* (*Carballido & Sander, 2014*). Both postzygapophyses are missing, as is the neural spine. The lateral centropostzygapophyseal lamina (icpol) is robust and vertically directed.

Scapula. The left scapula is nearly complete, lacking only small portions of the proximal plate and distal expansion (CGS V001-5, Fig. 6), and is flat and elongate. The lateral and medial surfaces of the proximal plate are both shallowly excavated, but the acromial ridge that is present in most neosauropods (*Upchurch, Barrett & Dodson, 2004*) is lacking. The dorsoventral height of the strongly expanded proximal plate is estimated to be more than 50% of the total length of the scapula (about 0.6), as in mamenchisaurids and more advanced sauropods (*Upchurch, Barrett & Dodson, 2004*). The acromial process is moderately developed and its posterior margin is slightly convex , which is similar to the condition in *Lingwulong* (*Xu et al., 2018*), *Lapparentosaurus*, *Cetiosaurus* and *Patagosaurus* (*Upchurch & Martin, 2002; Holwerda, 2019*). Comparatively, the acromial process is better developed in mamenchisaurids (Fig. 7), but poorly developed in *Shunosaurus* (*Zhang, 1988*). The long, anteroventrally protruding glenoid region is transversely thick. The glenoid region is rectangular in lateral view, and bears a slightly rugose articular surface. The lateral and medial surfaces of the scapular blade are both convex, creating a lenticular cross section, although the convexity of the lateral surface is more pronounced. The blade is slightly deflected medially, relative to the proximal plate. The distal end of the blade is strongly expanded dorsoventrally, though the dorsal part of the expanded area is slightly damaged. The distal end of the scapular blade is also strongly expanded in *Omeisaurus*, *Mamenchisaurus*, *Yuanmousaurus* (*Lu et al., 2006*), *Cetiosaurus* (*Upchurch & Martin, 2002*), and *Patagosaurus* (*Holwerda, 2019*), but only slightly expanded in the early-diverging sauropods *Shunosaurus* (*Zhang, 1988*) and *Barapasaurus* (*Bandyopadhyay et al., 2010*), and in the diplodocoid *Lingwulong* (Fig. 7).

Discussion

The recovered bones of the new Tibetan sauropod dinosaur are generally similar to those of other Early and Middle Jurassic sauropods, and also preserve some derived features previously known in mamenchisaurids. The cervicals are opisthocoelous and short, as in the Early Jurassic sauropods *Kotasaurus* from India (*Yadagiri, 2001*), *Tazoudasaurus* from Morocco (*Allain & Aquesbi, 2008*), and *Zizhongosaurus* and *Gongxiansaurus* (which now can only be studied on the basis of information in the literature, because this specimen may have been destroyed due to exhibition hall collapsed) from the Sichuan Basin (*He et al., 1998; Xing et al., 2019*), as well as the middle Jurassic *Shunosaurus* (*Zhang, 1988*) and *Patagosaurus* (*Holwerda, Rauhut & Pol, 2021*). The lateral surfaces of the centra are excavated as in most sauropods, such as *Tonganosaurus* from the Lower Jurassic Yimen Formation of the Sichuan Basin (*Li et al., 2010*), but the cervicals of *Tonganosaurus* are more elongated and have no septa in their lateral excavations. The shallow concavity of the lateral surface of the axial centrum, together with the lateral excavations and ventral midline keels on the postaxial cervical centra, represent strong similarities to Middle Jurassic sauropods from the Sichuan Basin, such as *Shunosaurus* and *Dashanpusaurus* (*Zhang, 1988; Peng et al., 2005*), and also to *Patagosaurus* (*Holwerda, Rauhut & Pol, 2021*). In addition, the Tibetan sauropod bones display some features seen in mamenchisaurids and neosauropods, such as a relatively robust scapula with a strongly dorsoventrally expanded proximal plate. However, the Tibetan sauropod also lacks many derived features of mamenchisaurids, including a deep lateral excavation on the axis, elongated cervical vertebrae, cervical centra with three or more lateral excavations and no ventral midline keel, and bifurcate cervical neural spines (*Young & Zhao, 1972; He, Li & Cai, 1988; Ouyang & Ye, 2002; Ren et al., 2021*). Our analysis results in 78 most parsimonious trees with a length of 1223 (consistency index equals 0.373; retention index equals 0.702). The strict consensus tree supports referral of the Tibetan sauropod to Eusauropoda (Fig. S2), but a reduced consensus tree indicates that the Tibetan sauropod is the most positionally unstable OTU. The majority-rule consensus tree posits the Tibetan sauropod as more derived than *Shunosaurus*, but excludes it from Mamenchisauridae and Neosauropoda (Fig. S3).

It is difficult to ascribe the Tibetan sauropod specimen to any known sauropod species or genus. The shortness of the cervical vertebrae is a point of resemblance to *Shunosaurus*, but the vertebrae bear more complicated excavations than are present in that taxon. However, the complexity of the cervical excavations may be subject to ontogenetic variation in sauropods. While documented examples of ontogenetically-driven morphological changes in sauropods are scant, such changes have been reported in a few genera, including *Shunosaurus* (*Ma et al., 2022*), *Brachiosaurus* (*Carballido et al., 2012*), *Europasaurus* (*Carballido & Sander, 2014*) and *Barosaurus* (*Melstrom et al., 2016*). Information from these taxa implies that the pleurocoels of the cervical and dorsal vertebrae became more structurally complex, and the cervical centra more elongate, in older individuals. In particular, Carballido & Sander (2014) divided the ontogeny of *Europasaurus* into five stages, based on the degree to which pleurocoels and laminae were developed.

The new Tibetan sauropod specimen may be a juvenile, based on its relatively small size and the presence of visible neurocentral sutures (ncs, Figs. 3E, 4B, 5C). The axial centrum is about as long (126 mm) as a complete example of the same element in a *Shunosaurus* (125 mm, ZDM T5042) specimen (*Zhang, 1988*) which was estimated to have had a total body length of 11 m. The maximum length of the preserved scapula is estimated to be less than 70 cm (based on the scapular proportions of mamenchisaurids), making it much shorter than the scapulae of adult individuals of such early-diverging eusauropod taxa as *Shunosaurus* (90 cm, ZDM T5042) (*Zhang, 1988*) and *M. youngi* (119 cm, ZDM0083) (*Ouyang & Ye, 2002*). However, the scapula of the Tibetan sauropod is slightly larger than that of a recently described partial juvenile *Shunosaurus* skeleton (scapula length 57.4 cm) from the Middle Jurassic of Chongqing Municipality, China (CLGPR V00007) (*Ma et al., 2022*). The latter has a slender shaft and low acromial process as in adults of *Shunosaurus*, and in contrast to the condition in the Tibetan sauropod. Unfortunately, no cervical vertebrae are preserved in the juvenile *Shunosaurus*, and most of the ontogenetic variations that could be inferred based on this specimen pertained to limb bones which are not represented in the Tibetan material (*Ma et al., 2022*).

The lack of fusion of the neurocentral sutures in the preserved cervical vertebrae suggests the new Tibetan sauropod material represents a juvenile individual. Using the criteria established by Carballido & Sander (2014) (and assuming that the ontogeny of *Europasaurus* was similar to that of the presumably much more ancestral taxon represented by the Tibetan material), the new Tibetan sauropod specimen can be recognized as a "late immature" individual, as well-developed laminae and fossae are apparent in the cervical series but the cervical vertebrae are still short. Similarly, the juvenile holotype of *Daanosaurus* from the Upper Jurassic of the Sichuan Basin has a very short axis (*Ye, Gao & Jiang, 2005*), and juvenile specimens of *Bellusaurus* from the Middle Jurassic of Xinjiang Autonomous Region have relatively short cervicals that bear deep excavations divided by septa, although in the *Bellusaurus* material the cervicals lack ventral midline keels and the scapulae are relatively slender (*Dong, 1990*). These comparisons indicate that the cervical vertebrae of the Tibetan sauropod would likely have developed more complex excavations and increased in size relative to other parts of the skeleton if ontogeny had continued, suggesting that an adult of the same species would have been more similar to mamenchisaurids (*Carballido & Sander, 2014*).

To summarize, the new Tibetan sauropod specimen displays a unique combination of features not seen in other early-diverging sauropods. However, more material is needed before a new taxon can be established, due to the incompleteness of the preserved bones and their juvenile status. The similarities between the Tibetan specimen and mamenchisaurids, which are already known to have a wide distribution in the Middle Jurassic of Asia (*Ren et al., 2021*), suggest that the Tibetan specimen may be at least closely related to Mamenchisauridae, particularly when possible ontogenetic effects are taken into account. A detailed study of ontogenetic variation in mamenchisaurids would be helpful in more confidently establishing the taxonomic position of the Tibetan specimen.

Conclusions

The Tibetan sauropod bones reveal the presence of a short-necked early-diverging sauropod in the Middle Jurassic Dongdaqiao Formation of Chaya County, Changdu District. Among previously described taxa, the specimen is most closely similar to early-diverging eusauropods from the Middle Jurassic, the resemblances including the shortness of the cervical centra and the fact that they bear lateral excavations. The specimen also possesses some derived features seen in the Late Jurassic mamenchisaurids and neosauropods, such as a robust scapula with a strongly dorsoventrally expanded proximal end, and a deep fossa on the lateral surface of the axial neural spine. The smallness of the available bones and the visible neurocentral sutures on the preserved cervicals suggest that the specimen represents a juvenile, which might have increased in relative neck length and the complexity of the pleurocoels and laminae in the cervical region if growth had continued. Therefore, an adult individual of the same species might show clearer similarities to mamenchisaurids. The new material provides significant information on the morphological transition from early-diverging eusauropods to mamenchisaurids, and expands the known diversity and biogeographic range of sauropods in the Middle Jurassic of East Asia.

Acknowledgements

We thank field team members Tao Yang and Yucong Ma for collecting these fossils, Xiaobing Wang from Tianyan Museum for preparing these fossils, and Xuefang Wei for very useful discussion. We thank the editor, Emanuel Tschopp, as well as Omar Rafael Regalado Fernandez, Femke Holwerda and an anonymous reviewer, for their very helpful comments on this manuscript.

References

Allain R, and Aquesbi N. 2008. Anatomy and phylogenetic relationships of *Tazoudasaurus naimi* (Dinosauria, Sauropoda) from the late Early Jurassic of Morocco. *Geodiversitas* 30:345-424.

An XY, Wang QY, Li Y, Wang BD, and Wang DB. 2021. New discovery of Jurassic dinosaur fossils in Chaya area, Qamdu district, Tibet [in Chinese with English abstract]. *Geological Bulletin of China* 40:189-193. DOI 10.12097/j.issn.1671-2552.2021.01.015

Bandyopadhyay S, Gillette DD, Ray S, and Sengupta DP. 2010. Osteology of *Barapasaurus tagorei* (Dinosauria: Sauropoda) from the Early Jurassic of India. *Palaeontology* 53:533-569. DOI 10.1111/j.1475-4983.2010.00933.x
Barrett PM, Chapelle KE, Staunton CK, Botha J, and Choiniere JN. 2019. Postcranial osteology of the neotype specimen of *Massospondylus carinatus* Owen, 1854 (Dinosauria: Sauropodomorpha) from the upper Elliot formation of South Africa. 53: 114-178.
Buffetaut E, Suteethorn V, Cuny G, Tong H, Le Loeuff J, Khansubha S, and Jongautchariyakul S. 2000. The earliest known sauropod dinosaur. *Nature* 407:72-74. DOI 10.1038/35024060
Carballido JL, Maromann JS, Schwarz-Wings D, and Pabst B. 2012. New information on a juvenile sauropod specimen from the Morrison Formation and the reassessment of its systematic position. *Palaeontology* 55:567-582. DOI: 10.1111/j.1475-4983.2012.01139.x
Carballido JL, and Sander PM. 2014. Postcranial axial skeleton of *Europasaurus holgeri* (Dinosauria, Sauropoda) from the Upper Jurassic of Germany: implications for sauropod ontogeny and phylogenetic relationships of basal Macronaria. *Journal of Systematic Palaeontology* 12:335-387. DOI: 10.1080/14772019.2013.764935
Dong ZM. 1990. On remains of the sauropods from Kelamaili region, Junggar Basin, Xinjiang, China [in Chinese with English abstract]. *Vertebrata PalAsiatica* 28:43-58. DOI 10.19615/j.cnki.1000-3118.1990.01.005
Goloboff PA, and Catalano SA. 2016. TNT version 1.5, including a full implementation of phylogenetic morphometrics. *Cladistics* 32:221-238. DOI 10.1111/cla.12160
Gomez K, Jose C, and Pol D. 2021. The axial skeleton of Bagualia alba (Dinosauria: Eusauropoda) from the Early Jurassic of Patagonia. *Palaeontologia electronica*. 24: a37. DOI 10.26879/1176
He XL, Li K, and Cai KJ. 1988. *The Middle Jurassic dinosaur fauna from Dashanpu, Zigong, Sichuan. Vol. IV. Sauropod dinosaurs (2), Omeisaurus tianfuensis*. Chengdu: Sichuan Scientific and Technological Publishing House.
He XL, Wang CS, Liu SZ, Zhou FY, Liu TQ, Cai KJ, and Dai B. 1998. A new sauropod dinosaur from the Early Jurassic in Gongxian County, South Sichuan [in Chinese with English abstract]. *Acta Geologica Sichuan* 18:1-6.
Holwerda FM. 2019. Revision of basal sauropods from the Middle Jurassic of Patagonia and the early evolution of sauropods. D. Phil. Thesis, Ludwig-Maximilians-Universität München.
Holwerda FM, Rauhut OWM, and Pol D. 2021. Osteological revision of the holotype of the Middle Jurassic sauropod dinosaur *Patagosaurus fariasi* Bonaparte, 1979 (Sauropoda: Cetiosauridae). *Geodiversitas* 43:575-643. DOI 10.5252/geodiversitas2021v43a16
Kutty T, Chatterjee S, Galton P, and Upchurch P. 2007. Basal sauropodomorphs (Dinosauria: Saurischia) from the Lower Jurassic of India: Their anatomy and relationships. *Journal of Paleontology* 81:1218-1240. DOI 10.1666/04-074.1
Li K. 1998. The sauropoda fossils and their stratigraphical distribution in China [in Chinese with English abstract]. *Journal of Chengdu University of Technology* 25:54-60.
Li K, Yang CY, Liu J, and Wang ZX. 2010. A new sauropod from the Lower Jurassic of Huili, Sichuan, China. *Vertebrata PalAsiatica* 48:185-202. DOI 10.19615/j.cnki.1000-3118.2010.03.002

Lu JC, Li SX, Ji Q, Wang GF, Zhang JH, and Dong ZM. 2006. New eusauropod dinosaur from Yuanmou of Yunnan Province, China. *Acta Geologica Sinica (English Edition)* 80:1-10. DOI 10.1111/j.1755-6724.2006.tb00788.x

Ma QY, Dai H, Tan C, Li N, Wang P, Ren XX, Meng L, Zhao Q, Wei G, and Xu X. 2022. New *Shunosaurus* (Dinosauria: Sauropoda) material from the Middle Jurassic Lower Shaximiao Formation of Yunyang, Chongqing, China. *Historical Biology* 34:1085-1099. DOI 10.1080/08912963.2021.1962852

Maidment SCR, and Wei GB. 2006. A review of the Late Jurassic stegosaurs (Dinosauria, Stegosauria) from the People's Republic of China. *Geological Magazine* 143:621-634. DOI: 10.1017/s0016756806002500

McPhee BW, Yates AM, Choiniere JN, and Abdala F. 2014. The complete anatomy and phylogenetic relationships of *Antetonitrus ingenipes* (Sauropodiformes, Dinosauria): implications for the origins of Sauropoda. *Zoological Journal of the Linnean Society* 171:151-205. DOI 10.1111/zoj12127

Melstrom KM, D'Emic MD, Chure D, and Wilson JA. 2016. A juvenile sauropod dinosaur from the Late Jurassic of Utah, U.S.A., presents further evidence of an avian style air-sac system. *Journal of Vertebrate Paleontology* 36:e1111898. DOI: 10.1080/02724634.2016.1111898

Nicholl C, Mannion P, and Barrett P. 2018. Sauropod dinosaur remains from a new Early Jurassic locality in the Central High Atlas of Morocco. *Acta Palaeontologica Polonica* 63:147-157. DOI 10.4202/app.00425.2017

Ouyang H, and Ye Y. 2002. *The first mamenchisaurian skeleton with complete skull: Mamenchisaurus youngi*. Chengdu: Sichuan Publishing House of Science and Technology.

Peng GZ, Ye Y, Gao YH, Shu CK, and Jiang S. 2005. *Jurassic Dinosaur Faunas in Zigong*. Chengdu: Sichuan Renmin Press.

Pol D, Ramezani J, Gomez K, Carballido JL, Carabajal AP, Rauhut OWM, Escapa IH, and Cúneo NR. 2020. Extinction of herbivorous dinosaurs linked to Early Jurassic global warming event. *Proceedings of the Royal Society B: Biological Sciences* 287:20202310. DOI 10.1098/rspb.2020.2310

Rauhut O. 2003. Revision of *Amygdalodon patagonicus* Cabrera, 1947 (Dinosauria, Sauropoda). *Mitteilungen aus dem Museum für Naturkunde in Berlin - Geowissenschaftliche Reihe* 6:173-181. DOI 10.1002/mmng.20030060110

Remes K, Ortega F, Fierro I, Joger U, Kosma R, Marín JM, Ide O, and Maga A. 2009. A new basal sauropod dinosaur from the Middle Jurassic of Niger and the early evolution of Sauropoda. *PLOS ONE* 4:e6924. DOI 10.1371/journal.pone.0006924

Ren XX, Sekiya T, Wang T, Yang ZW, and You HL. 2021. A revision of the referred specimen of *Chuanjiesaurus anaensis* Fang et al., 2000: a new early branching mamenchisaurid sauropod from the Middle Jurassic of China. *Historical Biology* 33:1872-1887. DOI: 10.1080/08912963.2020.1747450

Upchurch P. 1998. The phylogenetic relationships of sauropod dinosaurs. *Zoological Journal of the Linnean Society* 124:43-103. DOI 10.1111/j.1096-3642.1998.tb00569.x

Upchurch P, Barrett PM, and Dodson P. 2004. Sauropoda. In: Weishampel DB, Peter D, and Osmólska H, eds. *The Dinosauria (second edition)*. Berkeley: University of California Press, 259-322.

Upchurch P, and Martin J. 2002. The Rutland *Cetiosaurus*: The anatomy and relationships of a Middle Jurassic British sauropod dinosaur. *Palaeontology* 45:1049-1074. DOI 10.1111/1475-4983.00275

Wang XF, and Chen XH. 2005. Stratigraphic Division and Comparison of Different Geological Ages in China. Beijing: Geological Publishing House (in Chinese). p 596.

Wedel MJ. 2003. The evolution of vertebral pneumaticity in sauropod dinosaurs. *Journal of Vertebrate Paleontology* 23:344-357. DOI 10.1671/0272-4634(2003)023[0344:TEOVPI]2.0.CO;2

Wilson JA. 2002. Sauropod dinosaur phylogeny: critique and cladistic analysis. *Zoological Journal of the Linnean Society* 136:215-275. DOI:10.1046/j.1096-3642.2002.00029.x

Wilson JA, and Upchurch P. 2009. Redescription and reassessment of the phylogenetic affinities of *Euhelopus zdanskyi* (Dinosauria: Sauropoda) from the Early Cretaceous of China. *Journal of Systematic Palaeontology* 7:199-239. DOI: 10.1017/S1477201908002691

Xing LD, Harris JD, and Currie PJ. 2011. First record of dinosaur trackway from Tibet, China. *Geological Bulletin of China* 30:173-178.

Xing LD, Lockley MG, Zhang LZ, Klein H, Zheng YW, Peng GZ, Jiang S, Dai L, and Burns ME. 2019. First Jurassic dinosaur tracksite from Guizhou Province, China: morphology, trackmaker and paleoecology. *Historical Biology* 31:1423-1432. DOI 10.1080/08912963.2017.1326485

Xing LD, Xu X, Lockley MG, Klein H, Zhang LJ, Persons WS, Wang DH, Wang MY, and Wan XQ. 2021. Sauropod trackways from the Middle Jurassic Chaya Group of Eastern Tibet, China. *Historical Biology* 33:3141-3151. DOI 10.1080/08912963.2020.1851687

Xu X, Upchurch P, Mannion PD, Barrett PM, Regalado-Fernandez OR, Mo J, Ma J, and Liu H. 2018. A new Middle Jurassic diplodocoid suggests an earlier dispersal and diversification of sauropod dinosaurs. *Nature Communications* 9:2700. DOI 10.1038/s41467-018-05128-1

Yadagiri P. 2001. The osteology of *Kotasaurus yamanpalliensis*, a sauropod dinosaur from the Early Jurassic Kota Formation of India. *Journal of Vertebrate Paleontology* 21:242-252. DOI: 10.1671/0272-4634(2001)021[0242:TOOKYA]2.0.CO;2

Yang ZJ, and Dong ZM. 1972. *Mamenchisaurus hochuanensis sp. nov.* Beijiing, China: Science Press.

Ye Y, Gao Y, and Jiang S. 2005. A new genus of Sauropod from Zigong, Sichuan. *Vertebrata Palasiatica* 43:175-181. DOI 10.19615/j.cnki.1000-3118.2005.03.002

Young CC, and Zhao XJ. 1972. *Mamenchisaurus hochuanensis*. *Institute of Vertebrate Paleontology and Paleoanthropology Monograph Series I* 8:1-30.

Zhang QN, You HL, Wang T, and Chatterjee S. 2018. A new sauropodiform dinosaur with a 'sauropodan' skull from the Lower Jurassic Lufeng Formation of Yunnan Province, China. *Scientific Reports* 8:13464. DOI 10.1038/s41598-018-31874-9

Zhang XQ, Li DQ, Xie Y, and You HL. 2020. Redescription of the cervical vertebrae of the Mamenchisaurid Sauropod *Xinjiangtitan shanshanesis* Wu et al. 2013. *Historical Biology* 32:803-822. DOI 10.1080/08912963.2018.1539970

Zhang YH. 1988. *The Middle Jurassic dinosaur fauna from Dashanpu, Zigong, Sichuan: sauropod dinosaurs (1) Shunosaurus*. Chengdu, China: Sichuan Publishing House of Science and Technology.

Zhao XJ. 1983. Phylogeny and evolutionary stages of Dinosauria. *Acta Palaeontologica Polonica* 28:295-306.

Zhao XJ. 1985. The Jurassic reptile fauna of China. In: Wang S, ed. *The Jurassic System of China*. Beijing: Geological Publishing House, 286-291.

Figure 1

Geologic map and stratigraphyic layer of sauropod remains in this study.

(A) Location of the Chaya area, Changdu District, where the material described in this paper was collected; (B). Lithostratigraphic column of the Dongdaqiao Formation in the study area.

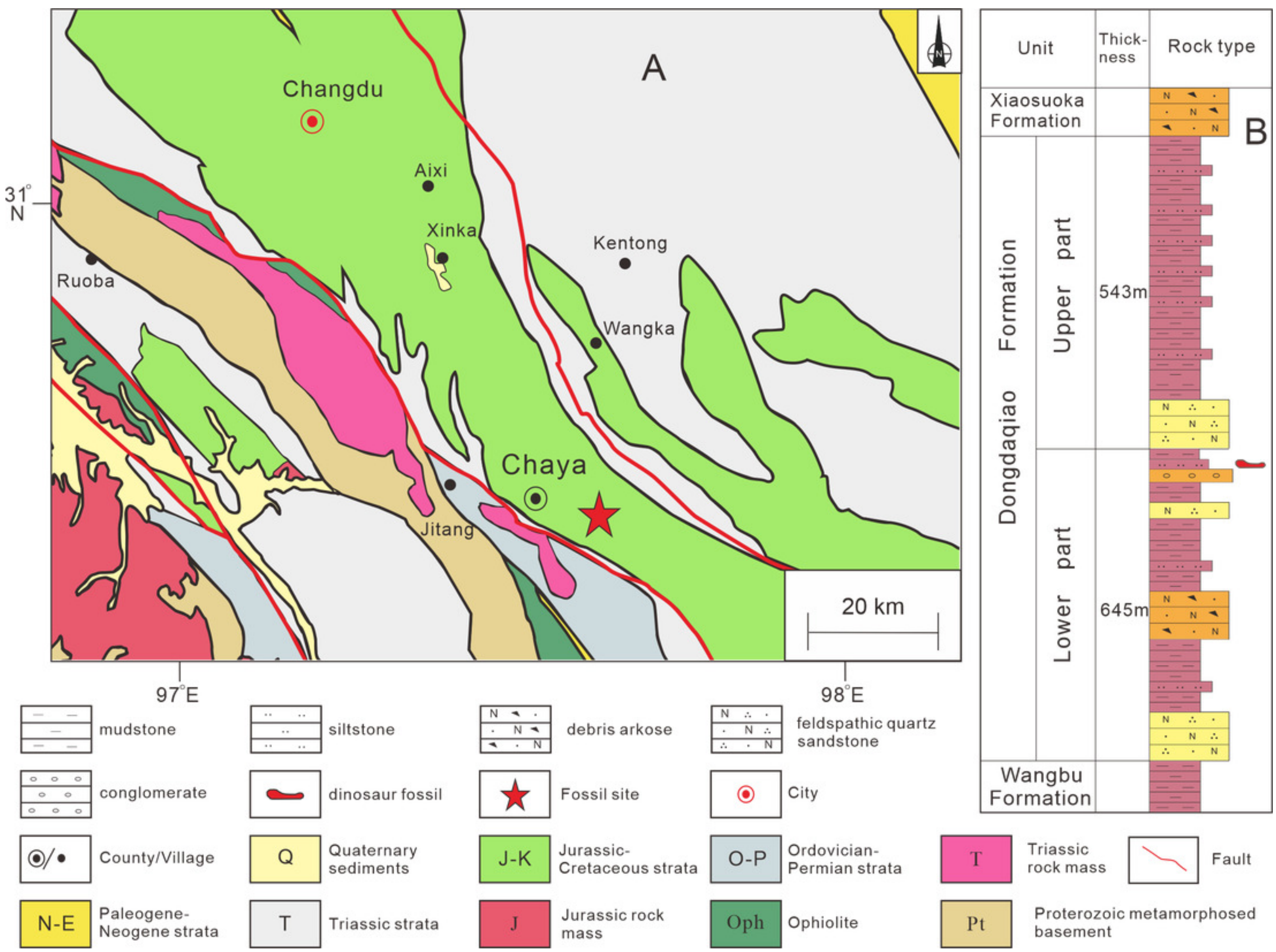

Figure 2

Axis of the Tibetan sauropod.

(A) Left lateral view; (B) Right lateral view; (C) Anterior view; (D) Dorsal view; (E) Ventral view; (F) Posteroventral view. **Abbreviations**: **di**, diapophysis; **epi**, epipophysis; **ic**, intercentrum; **nc**, neural canal; **ns**, neural spine; **podl**, postzygodiapophyseal lamina; **poz**, postzygapophysis; **pp**, parapophysis; **sdf**, spinodiapophyseal fossa; **spof**, spinopostzygapophyseal fossa; **spol**, spinopostzygapophyseal lamina.

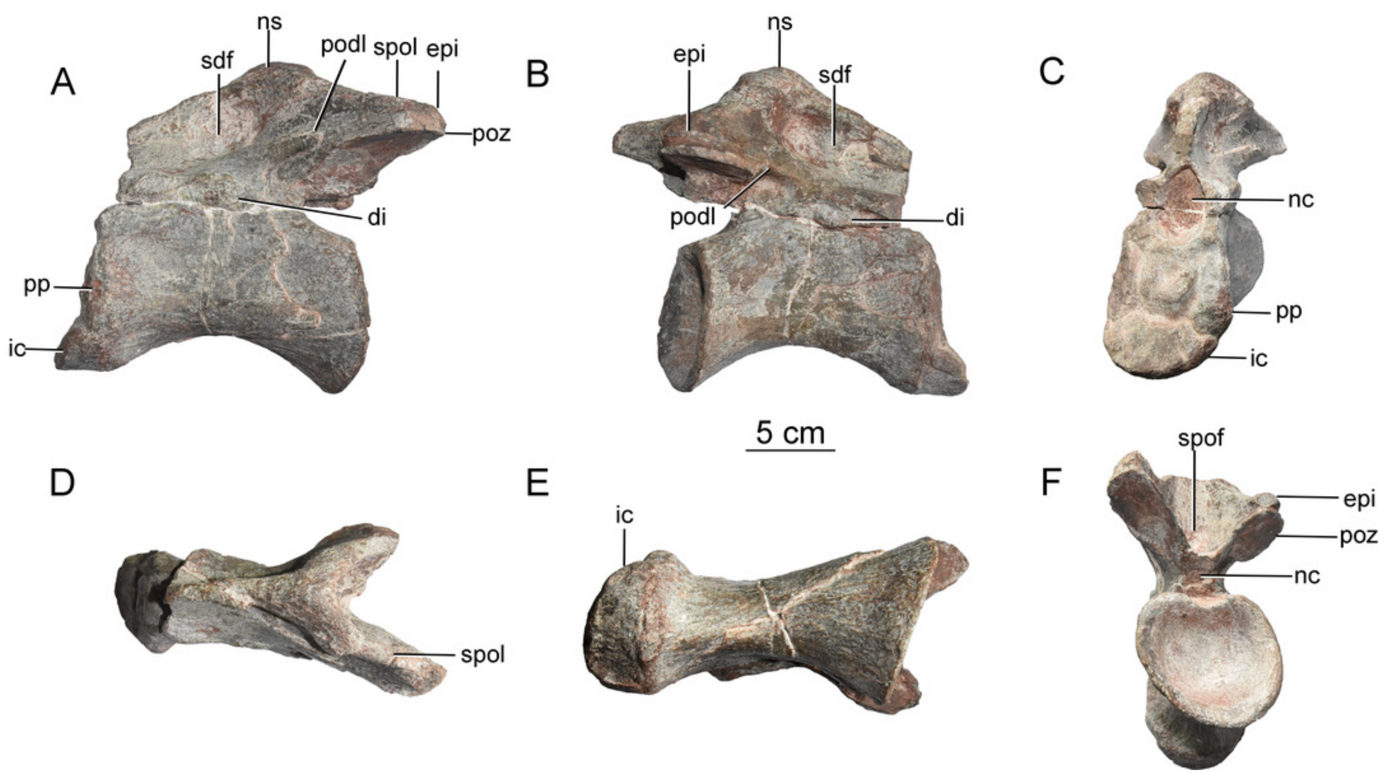

Figure 3

Possible anterior cervical vertebra of the Tibetan sauropod.

(A) Right lateral view; (B) Left lateral view; (C) Ventral view ; (D) Dorsal view; (E) Anterior view; (F) Posterior view. **Abbreviations**: **agr**, anterior neural spine groove; **acdl**, anterior centrodiapophyseal lamina; **cprl**, centroprezygapophyseal lamina; **dp**, diapophysis; **fo**, fossa; **tprl**, intraprezygapophyseal lamina; **nc**, neural canal; **ncs**, neurocentral suture; **ns**, neural spine; **pl**, pleurocoel; **plr**, pleurocoel ridge; **pcdl**, posterior centrodiapophyseal lamina; **podl**, postzygodiapophyseal lamina; **prdl**, prezygodiapophyseal lamina; **sprl**, spinoprezygapophyseal lamina; **vk**, ventral keel.

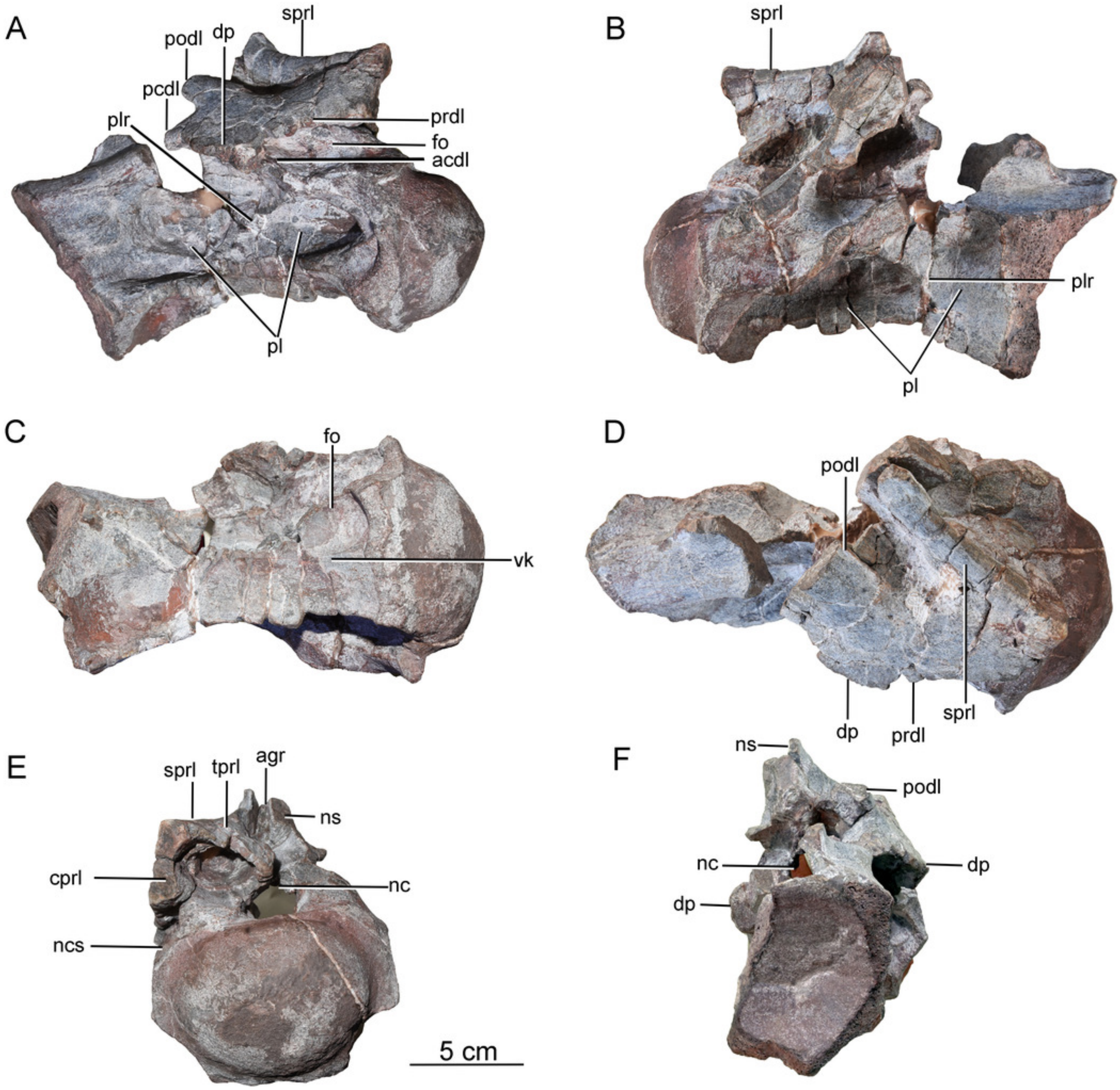
A
podl
dp
sprl
pcdl
plr
prdl
fo
acdl
pl
B
sprl
plr
pl
C
fo
vk
D
podl
dp
prdl
sprl
E
sprl
tprl
agr
ns
cprl
nc
ncs
5 cm
F
ns
podl
nc
dp
dp

Figure 4

Possible mid-cervical vertebra of the Tibetan sauropod.

(A) Right lateral view; (B) Left lateral view; (C) Posterior view; (D) Ventral view; (E) Anterior view. **Abbreviations**: **agr**, anterior neural spine groove; **cdl**, centrodiapophyseal lamina; **dp**, diapophysis; **nc**, neural canal; **ncs**, neurocentral suture; **ns**, neural spine; **pl**, pleurocoel; **plr**, pleurocoel ridge; **podl**, postzygodiapophyseal lamina; **ppr**, posterior process; **prdl**, prezygodiapophyseal lamina; **spol**, spinopostzygapophyseal lamina; **sprl**, spinoprezygapophyseal lamina

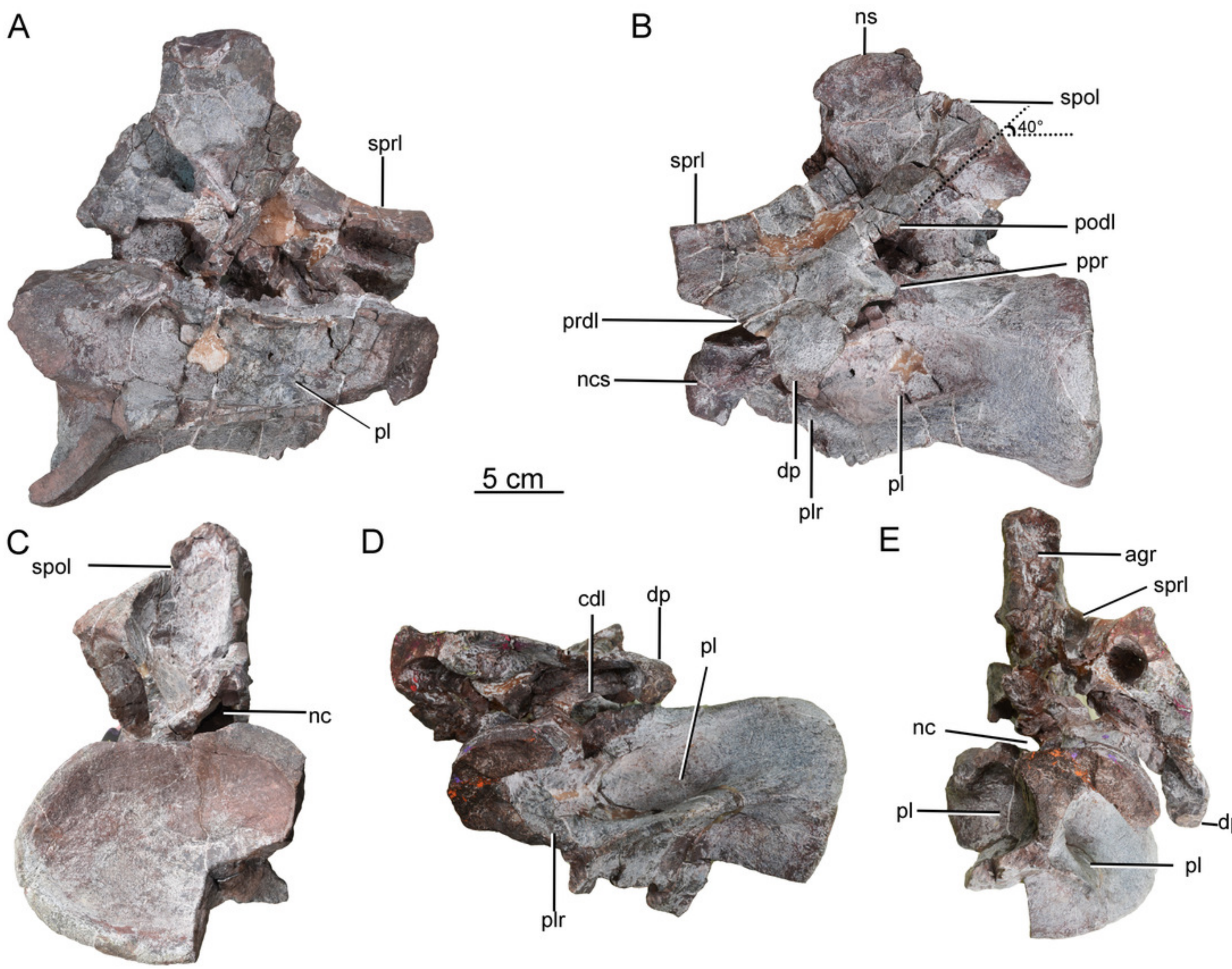

Figure 5

Possible posterior cervical vertebra of the Tibetan sauropod

(A) Right lateral view; (B) Left lateral view; (C) Anterior view; (D) Ventral view; (E) Dorsal view; (F) Posterior view. **Abbreviations**: **acdl**, anterior centrodiapophyseal lamina; **cprl**, centroprezygapophyseal lamina; **dp**, diapophysis; **dlc**, dorsal lamina of the centrum; **fo**, fossa; **lcpol**, lateral centropostzygapophyseal lamina ; **nc**, neural canal; **ncs**, neurocentral suture; **pcdl**, posterior centrodiapophyseal lamina; **pl**, pleurocoel; **podl**, postzygodiapophyseal lamina; **pp**, parapophysis; **prdl**, prezygodiapophyseal lamina; **sprl**, spinoprezygapophyseal lamina; **vk**, ventral keel

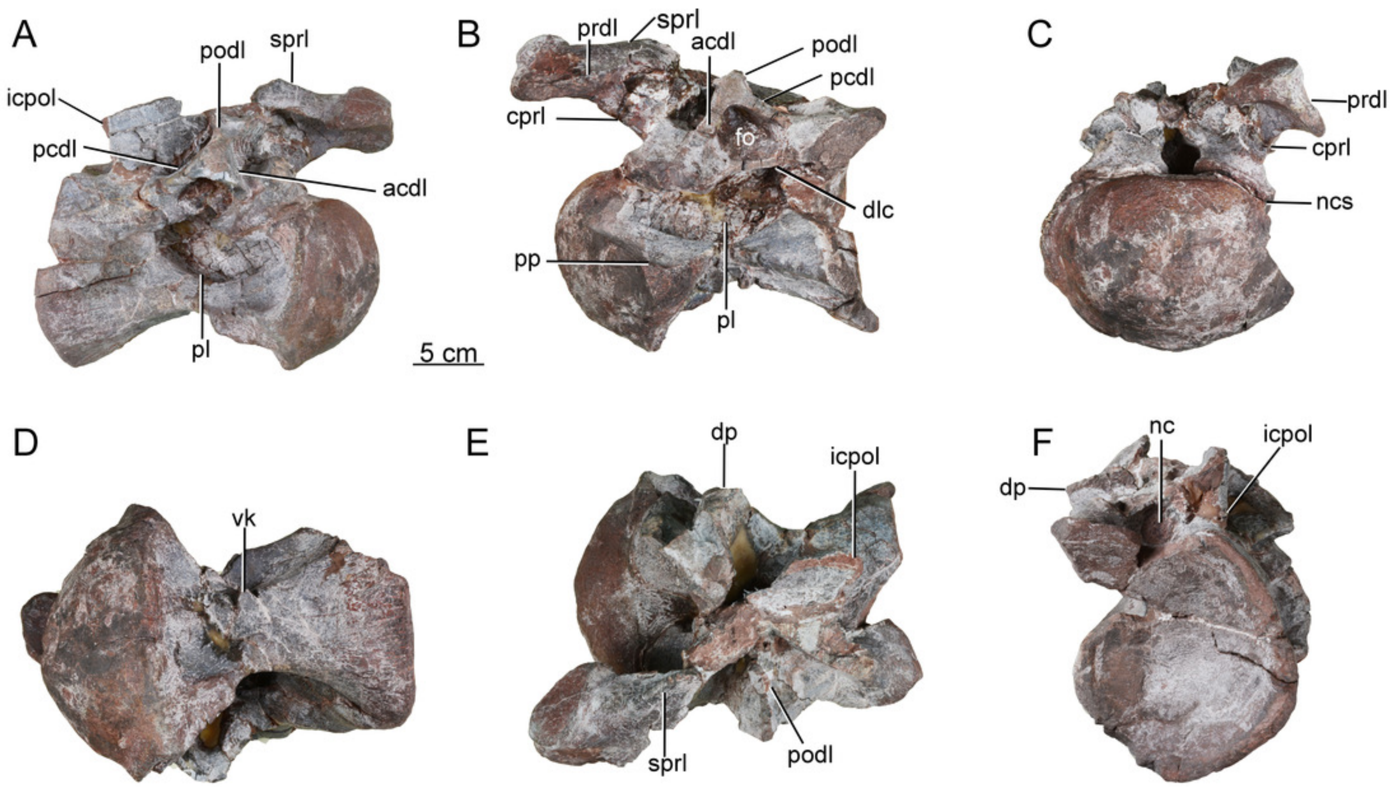

Figure 6

Left scapula of the Tibetan sauropod.

(A) Lateral view; (B) Medial view; (C) Ventral view; (D) Dorsal view; (E) Posterior view; (F) Anterior view. **Abbreviations**: **ac**, acromial process; **gl**, glenoid

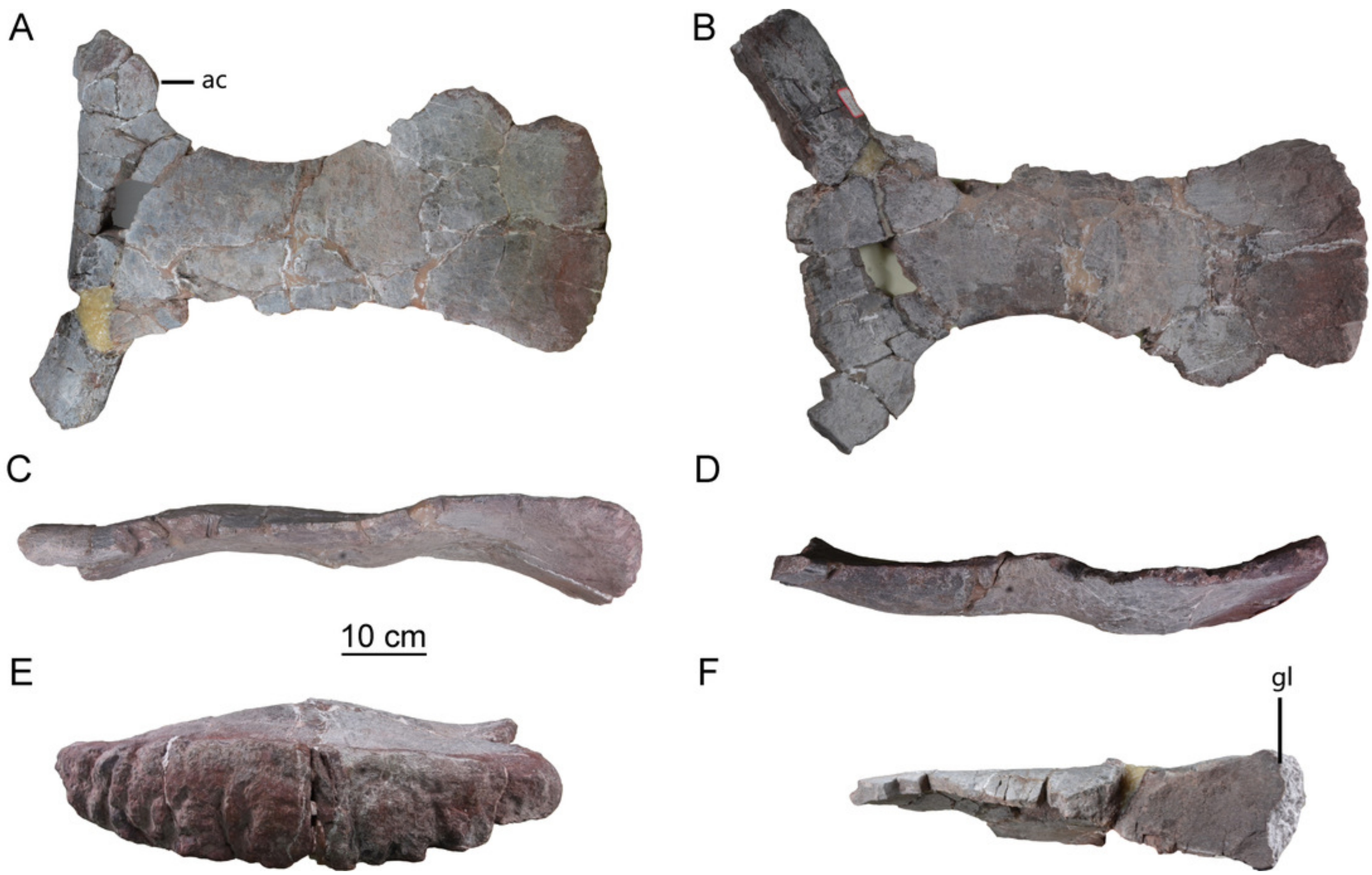

Figure 7

Comparison of left scapulae in lateral view

(A) *Tonganosaurus hei* (MCDUT 14454, reversed); (B) *Shunosaurus lii* (ZDM T 5402); (C) Tibetan sauropod (CGS V001); (D) *Lingwulong shenqi* (LM V001b, reversed); (E) *Omeisaurus tianfuensis* (ZDM T5704); (F) *Mamenchisaurus youngi* (ZDM0083). **Abbreviations**: **ac**, acromial process; **gl**, glenoid

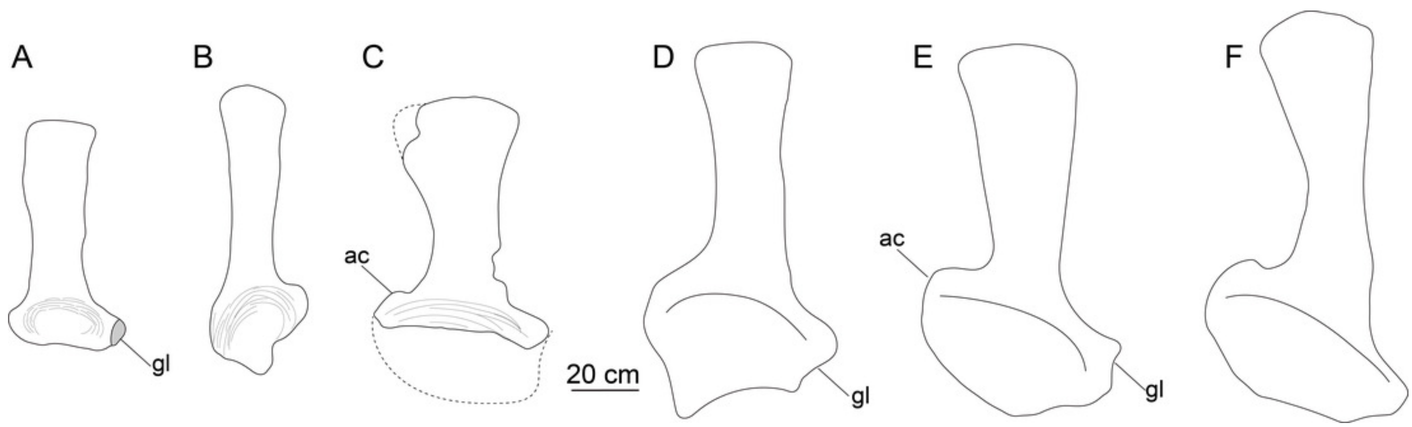

Table 1(on next page)

Measurements of Tibetan sauropod bones.

Table 1. Measurements of Tibet sauropod bones.

Elements	Dimension	Measurements (mm)
Axis(CGS V001-1)	1 Centrum length	126.09
	2 Anterior centrum height	92.89
	3 Anterior centrum width	67.66
	4 Centrum height at the mid region	65.37
	5 Centrum width at the mid region	N/A
	6 Posterior centrum height	78.29
	7 Posterior centrum width	85.10
	8 Neural arch length (shortest)	98.03
	9 Neural arch height	84.26
	10 Neural arch width (anterior end)	48.12
	11 Neural canal width (anterior end)	29.82
	12 Neural canal height (anterior end)	45.25
	13 Neural canal width (posterior end)	24.52
	14 Neural canal height (posterior end)	24.66
	15 Neural arch width (posterior end)	45.17
	Ratio of centrum length to posterior centrum height	1.61
	Ratio of centrum length to posterior centrum width (EI)	1.48
	Ratio of centrum length to the average of posterior centrum width (aEI)	1.54
Cervical (CGS V001-2)	1 Centrum length (including ball)	196.07
	2 Centrum length (excluding ball)	153.55
	3 Anterior condyle height	71.60
	4 Anterior condyle width	86.85
	5 Anterior centrum height	78.07
	6 Anterior centrum width	110.67
	7 Centrum height at the mid region	61.85
	8 Centrum width at the mid region	N/A
	9 Posterior centrum height	103.15
	10 Preserved (estimated) posterior centrum width	68.35 (105*)
	11 Anterior pneumatopore length	71.44
	12 Anterior pneumatopore height	30.38
	13 Posterior pneumatopore length	40.65
	14 Posterior pneumatopore height	40.57
	15 Neural arch length (shortest)	141.73
	16 Neural arch height	79.97
	17 Neural arch width (mid region)	83.98
	18 Neural canal width (anterior end)	27.40

	19 Neural canal height	18.35
	Ratio of centrum length to posterior centrum height	1.90
	EI value	1.9*
	aEI value	1.9*
Cervical (CGS V001-3)	1 Preserved (estimated) centrum length	252.06 (300*)
	2 Centrum height at the mid region	125.79
	3 Posterior centrum height	123.06
	4 Preserved (estimated) posterior centrum width	159.67 (165*)
	5 Posterior pneumatopore length	131.17
	6 Posterior pneumatopore height	55.66
	7 Neural arch length (shortest)	144.26
	8 Neural arch height (including neural spine)	186.55
	9 Neural spine height	51.64
	10 Neural spine width (anteroposterior)	66.15
	11 Neural spine thickness (transverse)	37.46
	12 Neural canal width (posterior end)	30.09
	13 Neural canal height (posterior end)	30.55
	Ratio of centrum length to posterior centrum height	2.4*
	EI value	1.8*
	aEI value	2.1*
Cervical (CGS V001-4)	1 Centrum length (including ball)	263.65
	2 Centrum length (excluding ball)	175.57
	3 Anterior condyle height	141.64
	4 Anterior condyle width	176.65
	5 Anterior centrum height	143.00
	6 Anterior centrum width	176.93
	7 Centrum height at the mid region	107.73
	8 Centrum width at the mid region	/
	9 Posterior centrum height	156.90
	10 Posterior centrum width	160*
	11 Right pneumatopore length	102.02
	12 Right pneumatopore height	56.68
	13 Left pneumatopore length	117.55
	14 Left pneumatopore height	51.94
	15 Neural arch length (shortest)	150.17
	16 Neural arch height	141.48
	17 Neural arch width (mid region)	158.91
	18 Anterior neural canal width (posterior end)	30.88
	19 Anterior neural canal height	42.26
	20 Posterior neural canal width (posterior end)	31.46
	21 Posterior neural canal height	33.12

	Ratio of centrum length to posterior centrum height	1.68
	EI value	1.65
	aEI value	1.67
Scapula (CGS V001-5)	1 Dorsoventral width of the proximal end	518.44
	2 Dorsoventral width of the mid-region	186.55
	3 Preserved dorsoventral width of the distal end	283.83 (incomplete)
	4 Anteroposterior length	685.97
	5 Transverse width of the proximal end	51.50
	6 Transverse width of the mid-region	36.04
	7 Transverse width of the distal end	61.55
	8 Transverse width of the glenoid rim	119.60
	9 Anteroposterior length of the glenoid rim	103.58

* denotes values that have been estimated, based on measurements of the preserved parts of the centrum and comparisons with other cervicals.